

# DGCR8-dependent microRNA biogenesis is essential for skin development

Rui Yi<sup>a,b,1</sup>, H. Amalia Pasolli<sup>a,b</sup>, Markus Landthaler<sup>a,c</sup>, Markus Hafner<sup>a,c</sup>, Tolulope Ojo<sup>a,c</sup>, Robert Sheridan<sup>d</sup>, Chris Sander<sup>d</sup>, Donal O'Carroll<sup>e</sup>, Markus Stoffel<sup>f</sup>, Thomas Tuschl<sup>a,c</sup>, and Elaine Fuchs<sup>a,b,2</sup>

<sup>a</sup>Howard Hughes Medical Institute, <sup>b</sup>Laboratory of Mammalian Cell Biology and Development, and <sup>c</sup>Laboratory of RNA Molecular Biology, The Rockefeller University, New York, NY 10065; <sup>d</sup>Computational Biology Center, Memorial Sloan-Kettering Cancer Center, 1275 York Avenue, Box 460, New York, NY 10065; <sup>e</sup>Adriano Buzzati-Traverso Campus, European Molecular Biology Laboratory, Via Ramarini 32, 00016 Monterotondo, Italy; and <sup>f</sup>Institute of Molecular Systems Biology, Swiss Federal Institute of Technology, CH-8093 Zurich, Switzerland

Contributed by Elaine Fuchs, October 24, 2008 (sent for review August 22, 2008)

**MicroRNAs play important roles in animal development. Numerous conditional knockout (cKO) studies of *Dicer* have been performed to interrogate the functions of microRNA during mammalian development. However, because *Dicer* was recently implicated in the biogenesis of endogenous siRNAs in mammals, it raises the question whether the *Dicer* cKO defects can be attributable to the loss of microRNAs. Previously, we and others conditionally targeted *Dicer* and identified its critical roles in embryonic skin morphogenesis. Here, we focus explicitly on microRNAs by taking a parallel strategy with *Dgcr8*, encoding an essential component of the microprocessor complex that is exclusively required for microRNA biogenesis. With this comparative analysis, we show definitively that the *Dicer*- and *Dgcr8*-null skin defects are both striking and indistinguishable. By deep sequencing analysis of microRNA depletion in both *Dicer*- and *Dgcr8*-null skin, we demonstrate that most abundantly expressed skin microRNAs are dependent on both *Dicer* and DGCR8. Our results underscore a specific importance of microRNAs in controlling mammalian skin development.**

dicer | small RNAs

**M**icroRNAs are a class of small (19–25nt), noncoding RNAs essential for animal development (1–3). They regulate gene expression post-transcriptionally by guiding the RNA-induced silencing complex (RISC) to their cognate sites at the 3'-untranslated region (UTR) of target mRNAs. Based on bioinformatics predictions, more than one third of mammalian mRNAs are potential targets of microRNAs (4). In the past several years, a two-step model of microRNA biogenesis has been widely validated (5). For most microRNAs, primary microRNA transcripts are first cropped into hairpin intermediates by a nuclear multiprotein Drosha-DGCR8 (Parsha) microprocessor complex (6, 7). Recently, an alternative mirtron pathway was reported where some intronic microRNA precursors can be processed by RNA splicing that bypasses the microprocessor cleavage (8–10). In either case, the processed microRNA precursors (pre-miRNA) are transported to the cytoplasm by exportin-5 (11, 12). After the transportation, mature microRNAs are then generated through enzymatic processing by another RNase III enzyme, *Dicer* (13, 14).

Because of the absolute requirement of *Dicer* for microRNA biogenesis, numerous conditional knockout (cKO) studies of *Dicer* have been performed to interrogate microRNA functions in mammalian development (1, 3). At a molecular level, a recent study has shown that in mouse embryonic stem (ES) cells, *Dicer* ablation results in depletion of all microRNAs (15). However, *Dicer* has also been reported to function in heterochromatin silencing of these cells (16), and in mouse oocytes, *Dicer* has been implicated in production of small RNA species other than microRNAs (17, 18).

In contrast to *Dicer*, DGCR8 function appears to be specific to microRNAs, because it acts in recognizing the pre-microRNA hairpin (19, 20). *Dgcr8* has also been targeted to mouse ES cells,

and although differentiation defects were similar to those of *Dicer*-null ES cells, *Dgcr8*-null ES cells appeared to grow faster than *Dicer*-null cells in the initial stages (16, 21, 22). The underlying basis for the differences in cultured ES cells is still uncertain, and the extent to which *Dicer* cKO developmental phenotypes in vivo are attributable explicitly to microRNAs has not been explored.

In the present study, we address this possibility directly by conditionally targeting *Dgcr8* in skin and comparing these mice to skin-specific *Dicer* mutant mice that we generated (23) (see also ref. 25). Our findings not only underscore the importance of microRNAs specifically in skin development, but also demonstrate that the striking defects in hair follicle and epidermal differentiation observed by the loss of *Dicer* function are primarily attributable to *Dicer*'s action on microRNAs.

## Results

***Dicer* and *Dgcr8* Skin Conditional Knockout Animals Show Indistinguishable Defects.** According to microarray gene profiling, *Dgcr8*, *Dicer*, and *Drosha* are expressed throughout all skin lineages, indicating their universal requirement in microRNA biogenesis (data not shown). We therefore generated mice harboring a conditional null *Dgcr8* allele as described (22) (Fig. 1A) and crossed them to mice expressing *keratin 14-Cre*, active in embryonic skin epithelial stem cells (24). To verify that *Dgcr8* and microRNA processing were effectively ablated in newborn (P0) skin epidermis, we used real-time quantitative PCR (qPCR) to quantify relative expression levels of three abundant skin microRNAs: miR-16, miR-203 and miR-205 (Fig. 1B). Having confirmed microRNA depletion in *Dgcr8* cKO skin, we characterized the mice.

Overall, the phenotype of *Dgcr8*<sup>fl/fl</sup>/*K14-Cre* cKO animals bore a striking resemblance to *Dicer*<sup>fl/fl</sup>/*K14-Cre* cKO mice (23, 25). Although indistinguishable to their WT littermates at birth, both mutants survived up to 5–6 days after birth (P5–P6) with rough skin and failed to gain weight compared with their WT littermates (Fig. 2A). Morphological and histological analyses revealed evaginating hair germs penetrating into and disrupting the epidermis, a hallmark of *Dicer* cKO skin (23, 25) (Fig. 2B). Immunolocalization confirmed that these structures were positive for Lef1, an essential hair germ marker. The local reduction

Author contributions: R.Y. designed research; R.Y., H.A.P., and T.O. performed research; R.Y., D.O., M.S., T.T., and E.F. contributed new reagents/analytic tools; R.Y., M.L., M.H., R.S., C.S., T.T., and E.F. analyzed data; and R.Y. and E.F. wrote the paper.

The authors declare no conflict of interest.

<sup>1</sup>Present address: University of Colorado at Boulder, 347 UCB, Department of Molecular, Cellular, and Developmental Biology, Boulder, CO 80309.

<sup>2</sup>To whom correspondence should be addressed at: Howard Hughes Medical Institute, Laboratory of Mammalian Cell Biology and Development, The Rockefeller University, 1230 York Avenue, Box 300, New York, NY 10065. E-mail: fuchs@rockefeller.edu.

This article contains supporting information online at [www.pnas.org/cgi/content/full/0810766105/DCSupplemental](http://www.pnas.org/cgi/content/full/0810766105/DCSupplemental).

© 2008 by The National Academy of Sciences of the USA



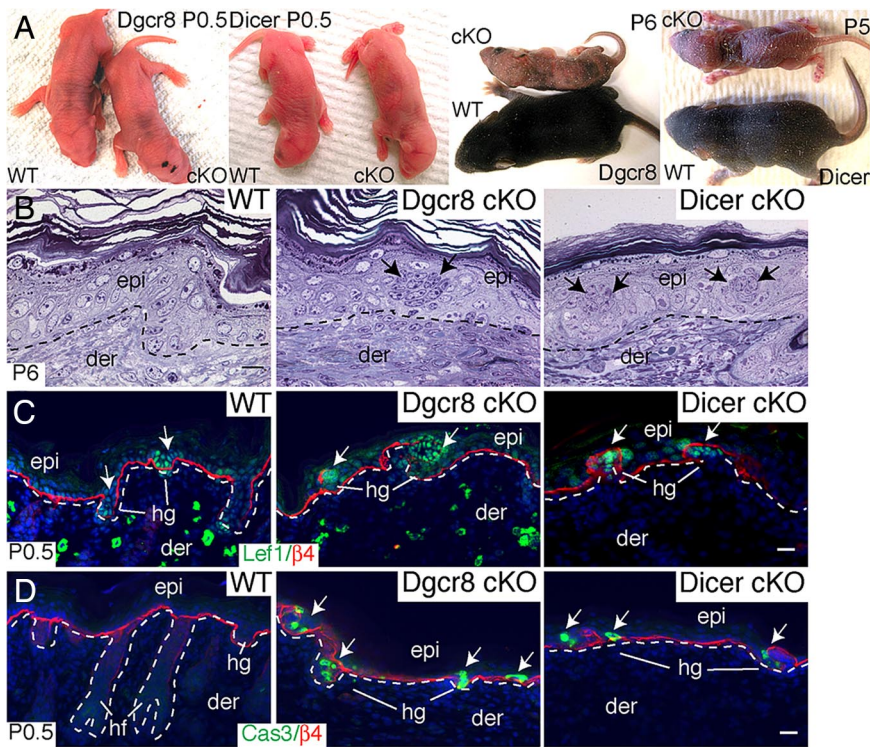


**Fig. 2.** Skin phenotypes of *Dgcr8* and *Dicer* cKO mice are strikingly similar. (A) *Dgcr8* and *Dicer* cKO mice can survive up to 5–6 days after birth. Newborn (P0.5) cKO and WT mice are similar in size and appearance. Thereafter, cKO mice fail to gain weight and exhibit taunted, flaky skin, a sign of severe dehydration. (B) P6 *Dgcr8* and *Dicer* cKO skins display evaginating hair germs (hg) that appear as balls of undifferentiated cells (arrows) that distort the epidermis (epi). (Scale bar, 10  $\mu$ m.) (C) Immunofluorescence identifies germs molecularly by transcription factor Lef1 and by hemidesmosomal  $\beta$ 4 integrin (nonspecific dermal staining is caused by the secondary antibody). (Scale bar, 20  $\mu$ m.) (D) Active caspase-3 (Cas3) denotes significant enrichment of apoptotic cells within hair germs in the cKO skin. Dotted lines mark epidermal-dermal boundaries. der, dermis. (Scale bar, 20  $\mu$ m.)

pleted, miR-21 showed an unusually high residual expression level ( $\approx 30\%$ ) in both cKO samples. Although this could arise from a very small contamination of nonskin cells robustly

expressing miR-21, it is also possible that the mature miR-21 has an unusually long half-life that could result in residual expression at P0 even though *K14-Cre* is strongly active by E14.5.

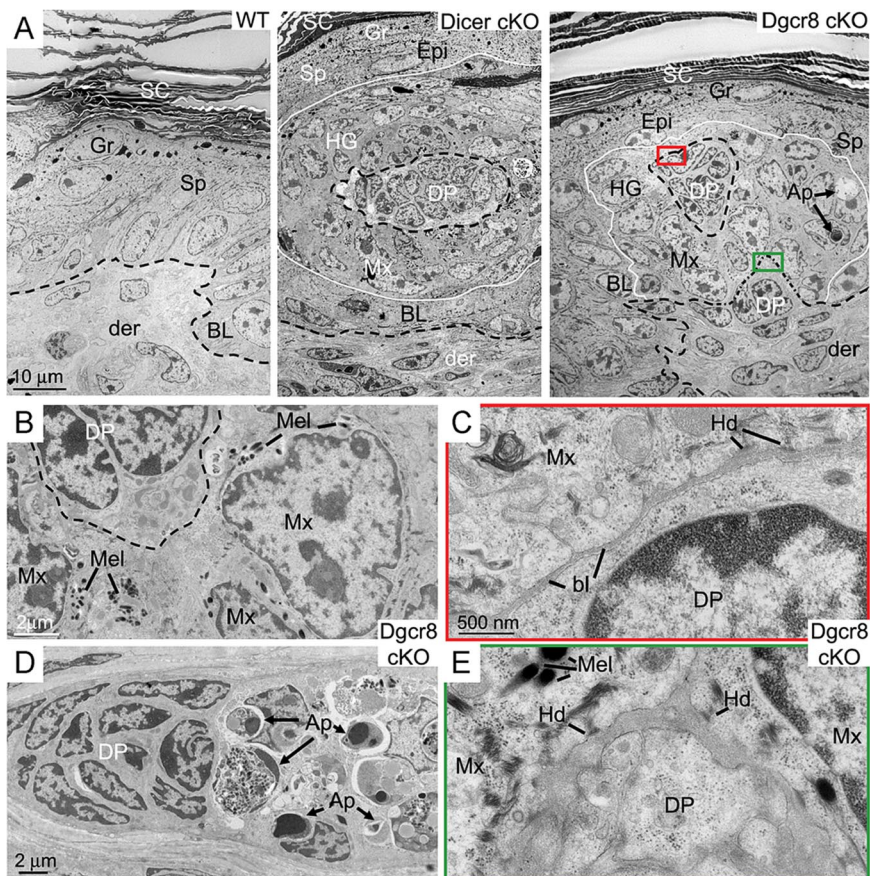


**Fig. 3.** Ultrastructural defects of *Dicer* and *Dgcr8* cKO skin. (A) Skins from neonatal WT control, *Dicer* cKO and *Dgcr8* cKO mice were fixed and processed for electron microscopy as described. Shown are regions of the epidermis, where a whorl of evaginated hair germ (hg) cells are readily identified by the presence of dermal papilla (DP) cells at the center of the structure. These aberrations in follicle morphogenesis distorted the surrounding epidermis. (Scale bar, 10  $\mu$ m.) (B) Cells with hair follicle matrix cell (Mx) morphology were present in the evaginating hair germs of *Dgcr8* cKO epidermis. These cells frequently contained melanin granules (Mel). Melanocytes are normally never in mouse skin epidermis, and the appearance of melanin within the whorls was an additional hallmark of the evaginating hair germs. (Scale bar, 2  $\mu$ m.) (C and E) Closed-up pictures of boxed areas in A. Note the presence of hemidesmosomes (Hd) and a loose basal lamina (bl) at the evaginating hair germ-DP border (C) as well as the epidermal-dermal boundary to what appeared to be an underlying DP (E) in the *Dgcr8* cKO skin. (Scale bar, 500 nm.) (D) Enriched apoptotic cells (Ap) in hair germs of *Dgcr8* cKO skin. (Scale bar, 2  $\mu$ m.) Additional abbreviations: SC, stratum corneum; Gr, granular layers; Sp, spinous layers; BL, basal epidermal layer; Der, dermis. Dotted lines mark epidermal-dermal boundaries.

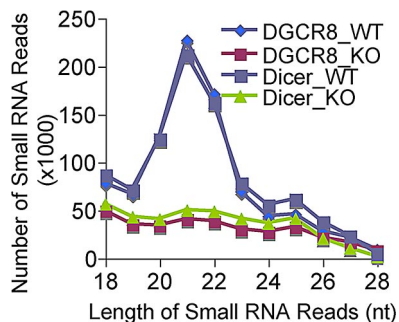


**Fig. 4.** Specific and similar depletion of small RNA reads (19–23 nt) in both *Dgcr8* and *Dicer* cKO skin. Small RNA reads from 18 to 28 nucleotides were charted from all four small RNA cDNA libraries. Note the nearly identical distribution patterns of small RNA reads within either two duplicate WT libraries or two cKO libraries.

Interestingly, miR-320 and miR-484 were highly expressed in the *Dgcr8* but not *Dicer*-deficient samples (Fig. 5*A* and Table S3). To confirm these distinctions with an alternative approach, we performed real-time qPCR to quantify the relative levels of the 67 most abundantly expressed microRNAs including miR-320 and miR-484 in skin. Consistent with our cloning results, 65 of these 67 microRNAs were depleted similarly in both *Dicer* and *Dgcr8* cKO, whereas miR-320 and miR-484 were depleted only in *Dicer* but not in the *Dgcr8* cKO skin (Fig. 5*B*). We also noticed that the expression of miR-320 was reported to be independent of DGCR8 in murine ES cells (22).

To probe how the biogenesis of miR-320 and miR-484 does not require DGCR8, we examined the secondary structure of their precursors predicted by miRBase (28). Although premiR-320 appeared to be a bona fide microRNA with the characteristic hairpin structure for the recognition by DGCR8 (19, 20, 29) (Fig. S2*A*), the annotated flanking sequence of miR-484 did not fold into the typical hairpin structure expected from a prototypical microRNA precursor (Fig. S2*B*). However, we noticed that the annotated flanking sequences of miR-484 do not completely overlap with the conserved sequences flanking mature miR-484 among vertebrates (Fig. S3*A*). Interestingly, when we used the conserved sequences flanking mature miR-484 (Fig. S3*B*) to predict the secondary structure of the miR-484 precursor by mfold (30), the resulted secondary structure showed the characteristic hairpin structure for prototypical microRNAs (Fig. S3*C*). Based on these data, we surmise that there may be additional features in miR-320 and miR-484 precursors that can allow their independence of DGCR8 recognition whereas the release of mature miR-320 and miR-484 from the hairpin is still dependent on Dicer.

Recently, an alternative mirtron pathway that does not require Drosha/DGCR8 processing was reported (8–10). However, we only recovered miR-877 and miR-1224, two of the most con-

**Table 1.** Cloning frequency of small non-coding RNAs from four epidermal libraries revealed the significant depletion only to the microRNA population in both *Dicer* and *Dgcr8* cKO samples

Sequence type	DGCR8_WT	DGCR8_KO	Dicer_WT	Dicer_5_KO
microRNA	373,467	12,071	325,707	8,070
rRNA	6,921	5,184	6,446	4,216
tRNA	9,623	8,618	10,623	6,097
sn/sno-RNA	990	1,012	798	482
calibration RNA	101	85	105	86
Total	391,102	26,970	343,679	18,951

The numbers are reads mapped to each small RNA species

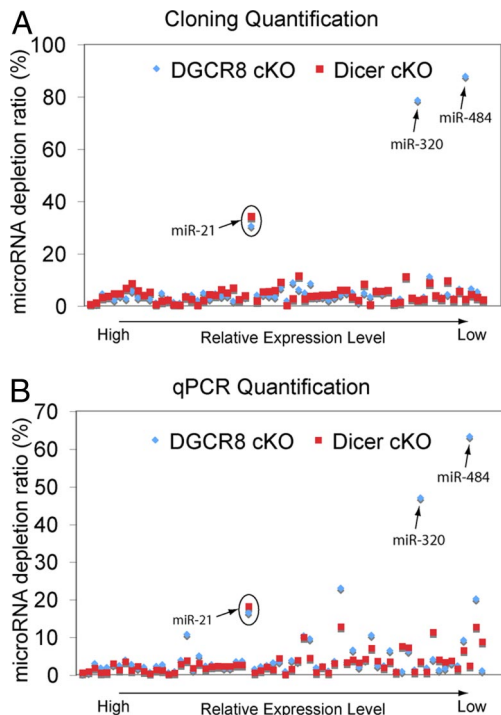


**Fig. 5.** Small RNA cloning and deep sequencing reveals the dependence of microRNA biogenesis on Dicer and DGCR8. (A) Compilation of microRNA sequencing data in *Dicer* and *Dgcr8* cKO samples compared with their WT littermate skins reveal similar dependence of microRNA biogenesis with the exception for miR-320 and miR-484, which require Dicer but not DGCR8. MiR-21 was depleted in both *Dicer* and *Dgcr8* cKO, but only partially ( $\approx 70\%$ , circle). MicroRNA depletion ratios were normalized against reads from rRNA, tRNA, and spiked-in calibration RNAs, none of which depends on Dicer or DGCR8. (B) qPCR microRNA expression validation of the cloning/sequencing results. Of 67 skin microRNAs subjected to quantification by qPCR, 65 were dependent similarly on Dicer and DGCR8. MiR-320 and miR-484 displayed dependency on Dicer but not DGCR8.

served and abundant mirtrons (10) in our libraries. The total reads for these two mirtron microRNAs were only 12 of 719,315 microRNA reads. This observation suggests that the mirtron pathway does not play a major role in microRNA biogenesis in skin.

## Discussion

Together, our phenotypic and small RNA profiling studies confirmed critical roles of microRNAs during mammalian skin development. Our deep sequencing analysis suggests that Dicer but not DGCR8 (the microprocessor complex) may be involved in the biogenesis of small RNAs, for example, endo-siRNA and sn/snoRNA-derived small RNAs in the skin. However, the indistinguishable phenotypic consequences of targeting *Dgcr8* or *Dicer* during embryonic skin development support the view that the primary function of both proteins is in processing of microRNAs. It is difficult to distinguish whether the skin differs in this respect from ES cells. It is formally possible that the reported growth-related differences between *Dicer* and *Dgcr8* null ES cells may be attributable not to differences in Dicer and DGCR8 function, but rather to variations in cell culture conditions and/or variations in procedures used by different groups to derive these mES lines (16, 21, 22).

Taken together our findings provide valuable insights into the relative importance of microRNAs and other small RNAs in a mammalian tissue in vivo. When contrasted against studies in mouse oocytes and ES cells, the lack of marked skin differences between *Dicer* and *Dgcr8* mutant mice suggest that different cell

types and/or tissues may differ in this regard. Future comparative studies of *Dicer* and *Dgcr8* cKO in other developmental systems, for example, hematopoiesis, myogenesis, and neurogenesis, should help in ascertaining the extent to which microRNAs dominate among other classes of small RNAs in regulating mammalian development.

## Materials and Methods

**Small RNA Cloning, Sequencing, and Annotation.** Total RNAs were isolated from newborn skin as described (23). Fifteen micrograms of total RNAs were used for the preparation of each library for Solexa sequencing as described (26). For each library, 0.01 fmol of each of the internal control oligonucleotides were added into the total RNA. Small RNA reads were matched against the known transcripts of known noncoding RNAs as described (31, 32). For the mapping of small RNA reads to mRNAs, small RNA reads that were perfectly matched to mouse mRNA (75,876 entries retrieved from GenBank) were scored. Data were shown when their total hits are >10 times in four libraries.

**Immunofluorescence and Antibodies.** OCT sections were fixed for 10 min in 4% PFA in PBS and washed three times for 5 min in PBS at RT. Immunofluorescence was performed as described (23). The primary antibodies used as the indicated

concentrations were: Lef1 (1:100, Fuchs Lab),  $\beta$ 4 Integrin ( $\beta$ 4, 1:100, BD Biosciences), Active Caspase-3 (1:1000, R&D Systems).

**Real-Time PCR Gene Expression Analysis.** MicroRNA real-time PCR quantification were performed by using the miScript system (Qiagen) according to the manufacturer's instruction. SnoRNA25 RNA were served as the internal control. The LightCycler 480 system was used for real-time PCR. Differences between samples and controls were calculated based on the  $2^{-\Delta\Delta C_P}$  method.

**Electron Microscopy.** Tissues were fixed for greater or equal than 1 h in 2% glutaraldehyde, 4% formaldehyde, and 2 mM  $\text{CaCl}_2$  in 0.05 M sodium cacodylate buffer, and then processed for Epon embedding. Samples were visualized with a Tecnai G2 transmission electron microscope.

**ACKNOWLEDGMENTS.** We thank E. Lai for comments and suggestions, N. Stokes, L. Polak, and D. Oristian for assistance in the mouse facility, S. Dewell for assistance with Solexa sequencing and data analysis, and A. Tarakhovskiy (The Rockefeller University, New York) for *Dicer*<sup>fl/fl</sup> mice. This work was supported by grants from the National Institutes of Health (NIH) and the Howard Hughes Medical Institute (E.F., T.T., and M.S.) and NIH Pathway to Independence Award K99AR054704 (to R.Y.). E.F. and T.T. are investigators of the Howard Hughes Medical Institute.

1. Stefani G, Slack FJ (2008) Small non-coding RNAs in animal development. *Nat Rev Mol Cell Biol* 9:219–230.
2. Bartel DP (2004) MicroRNAs: Genomics, biogenesis, mechanism, and function. *Cell* 116:281–297.
3. Bushati N, Cohen SM (2007) microRNA functions. *Annu Rev Cell Dev Biol* 23:175–205.
4. Lewis BP, Burge CB, Bartel DP (2005) Conserved seed pairing, often flanked by adenosines, indicates that thousands of human genes are microRNA targets. *Cell* 120:15–20.
5. Lee Y, et al. (2002) MicroRNA maturation: Stepwise processing and subcellular localization. *EMBO J* 21:4663–4670.
6. Denli AM, et al. (2004) Processing of primary microRNAs by the Microprocessor complex. *Nature* 432:231–235.
7. Gregory RI, et al. (2004) The Microprocessor complex mediates the genesis of microRNAs. *Nature* 432:235–240.
8. Okamura K, et al. (2007) The mirtron pathway generates microRNA-class regulatory RNAs in *Drosophila*. *Cell* 130:89–100.
9. Ruby JG, Jan CH, Bartel DP (2007) Intronic microRNA precursors that bypass Drosha processing. *Nature* 448:83–86.
10. Berezikov E, et al. (2007) Mammalian mirtron genes. *Mol Cell* 28:328–336.
11. Yi R, Qin Y, Macara IG, Cullen BR (2003) Exportin-5 mediates the nuclear export of pre-microRNAs and short hairpin RNAs. *Genes Dev* 17:3011–3016.
12. Lund E, et al. (2004) Nuclear export of microRNA precursors. *Science* 303:95–98.
13. Bernstein E, Caudy AA, Hammond SM, Hannon GJ (2001) Role for a bidentate ribonuclease in the initiation step of RNA interference. *Nature* 409:363–366.
14. Hutvagner G, et al. (2001) A cellular function for the RNA-interference enzyme Dicer in the maturation of the let-7 small temporal RNA. *Science* 293:834–838.
15. Calabrese JM, Seila AC, Yeo GW, Sharp PA (2007) RNA sequence analysis defines Dicer's role in mouse embryonic stem cells. *Proc Natl Acad Sci USA* 104:18097–18102.
16. Kanelloupolou C, et al. (2005) Dicer-deficient mouse embryonic stem cells are defective in differentiation and centromeric silencing. *Genes Dev* 19:489–501.
17. Tam OH, et al. (2008) Pseudogene-derived small interfering RNAs regulate gene expression in mouse oocytes. *Nature* 453:534–538.
18. Watanabe T, et al. (2008) Endogenous siRNAs from naturally formed dsRNAs regulate transcripts in mouse oocytes. *Nature* 453:539–543.
19. Han J, et al. (2006) Molecular basis for the recognition of primary microRNAs by the Drosha-DGCR8 complex. *Cell* 125:887–901.
20. Sohn SY, et al. (2007) Crystal structure of human DGCR8 core. *Nat Struct Mol Biol* 14:847–853.
21. Murchison EP, et al. (2005) Characterization of Dicer-deficient murine embryonic stem cells. *Proc Natl Acad Sci USA* 102:12135–12140.
22. Wang Y, et al. (2007) DGCR8 is essential for microRNA biogenesis and silencing of embryonic stem cell self-renewal. *Nat Genet* 39:380–385.
23. Yi R, et al. (2006) Morphogenesis in skin is governed by discrete sets of differentially expressed microRNAs. *Nat Genet* 38:356–362.
24. Vasioukhin V, Degenstein L, Wise B, Fuchs E (1999) The magical touch: Genome targeting in epidermal stem cells induced by tamoxifen application to mouse skin. *Proc Natl Acad Sci USA* 96:8551–8556.
25. Andl T, et al. (2006) The miRNA-processing enzyme dicer is essential for the morphogenesis and maintenance of hair follicles. *Curr Biol* 16:1041–1049.
26. Hafner M, et al. (2008) Identification of microRNAs and other small regulatory RNAs using cDNA library sequencing. *Methods* 44:3–12.
27. Pedersen JS, et al. (2006) Identification and classification of conserved RNA secondary structures in the human genome. *PLoS Comput Biol* 2:e33.
28. Griffiths-Jones S, Saini HK, van Dongen S, Enright AJ (2008) miRBase: Tools for microRNA genomics. *Nucleic Acids Res* 36:D154–D158.
29. Zeng Y, Yi R, Cullen BR (2005) Recognition and cleavage of primary microRNA precursors by the nuclear processing enzyme Drosha. *EMBO J* 24:138–148.
30. Zuker M (2003) Mfold web server for nucleic acid folding and hybridization prediction. *Nucleic Acids Res* 31:3406–3415.
31. Berninger P, Gaidatzis D, van Nimwegen E, Zavolan M (2008) Computational analysis of small RNA cloning data. *Methods* 44:13–21.
32. Landgraf P, et al. (2007) A mammalian microRNA expression atlas based on small RNA library sequencing. *Cell* 129:1401–1414.